

Evaluation of the forward Compton scattering off protons: Spin-independent amplitude

Oleksii Gryniuk,^{1,2} Franziska Hagelstein,¹ and Vladimir Pascalutsa¹¹*Institut für Kernphysik and PRISMA Cluster of Excellence, Johannes Gutenberg-Universität Mainz, D-55128 Mainz, Germany*²*Physics Department, Taras Shevchenko Kyiv National University, Volodymyrska 60, UA-01033 Kyiv, Ukraine*

(Received 2 September 2015; published 21 October 2015)

We evaluate the forward Compton scattering off the proton, based on Kramers-Kronig kind of relations which express the Compton amplitudes in terms of integrals of total photoabsorption cross sections. We obtain two distinct fits to the world data on the unpolarized total photoabsorption cross section and evaluate the various spin-independent sum rules using these fits. For the sum of proton electric and magnetic dipole polarizabilities governed by the Baldin sum rule, we obtain the following average (between the two fits): $\alpha_{E1} + \beta_{M1} = 14.0(2) \times 10^{-4} \text{ fm}^3$. An analogous sum rule involving the quadrupole polarizabilities of the proton is evaluated too. The spin-independent forward amplitude of proton Compton scattering is evaluated in a broad energy range. The results are compared with previous evaluations and the only experimental data point for this amplitude (at 2.2 GeV). We remark on sum rules for the elastic component of polarizabilities.

DOI: 10.1103/PhysRevD.92.074031

PACS numbers: 13.60.Fz, 14.20.Dh, 25.20.Dc, 11.55.Hx

I. INTRODUCTION

It is long known that the forward Compton scattering (CS) amplitudes can, by unitarity, causality, and crossing, be expressed through integrals of the photoabsorption cross sections [1]. The low-energy expansions of these expressions lead to a number of useful sum rules, most notably those of Baldin [2], and GDH [3,4]. Given the photoabsorption cross sections, one can, thus, provide a reliable assessment of some of the static electromagnetic properties of the nucleon and nuclei, as well as of the forward CS amplitudes in general. For the proton, the first such assessments were performed in the early 1970s [5,6]. Since then, the knowledge of the photoabsorption cross sections appreciably improved, and yet for the unpolarized case, only the Baldin sum rule has been updated [7–9]. In this work, we provide a reassessment of the forward spin-independent amplitude of proton CS and evaluate the associated sum rules involving the dipole and quadrupole polarizabilities of the proton.

Sum rules are essentially the only way to gain empirical knowledge of the forward CS amplitudes. It is impossible to access the forward kinematics in real CS experiments. The measurement of the forward spin-independent CS amplitude can be done indirectly through the process of dilepton photoproduction ($\gamma p \rightarrow p e^+ e^-$) [10]. The time-like CS involved in the process of dilepton photoproduction yields access to real CS given the small virtuality of the outgoing photon, or equivalently, the nearly vanishing invariant mass of the produced pair. The experimental result [10] compared well with the aforementioned evaluations [5,6]. Despite the substantial additions to the database of total photoabsorption cross sections, the works

of Damashek and Gilman (DG) [5] as well as Armstrong *et al.* [6] remained to be, until now, the only evaluations of the full amplitude.

The newer data were used, however, in the most recent evaluations of the Baldin sum rule [8,9], which yields the sum of the electric and magnetic dipole polarizabilities, Eq. (9). These recent analyses obtained a somewhat lower value for the sum than DG; cf. Table III. In this work, we find that the difference between the early and the recent evaluations arises from systematic inconsistencies in the experimental database. We also obtain the sum rule value for a combination of higher-order quadrupole polarizabilities and compare it with several theoretical predictions.

This paper is organized as follows. In Sec. II we give a brief overview of the Kramers-Kronig relation and sum rules for polarizabilities. In Sec. III we discuss the fitting procedure for the unpolarized total proton photoabsorption cross section data. The sum rule evaluations of scalar polarizabilities and of the spin-independent forward CS amplitude are presented in Sec. IV. Conclusions are given in Sec. V. The Appendix demonstrates the elastic-channel contribution to the sum rules and polarizabilities on the example of one-loop scalar QED.

II. FORWARD COMPTON AMPLITUDE AND SUM RULES

For a spin-1/2 target, such as the proton, the forward CS amplitude is given by

$$T_{fi} = f(\nu)\mathbf{\epsilon}'^* \cdot \mathbf{\epsilon} + g(\nu)i(\mathbf{\epsilon}'^* \times \mathbf{\epsilon}) \cdot \mathbf{\sigma}, \quad (1)$$

where f and g are scalar functions of the photon lab energy ν ; vectors $\boldsymbol{\epsilon}$ and $\boldsymbol{\sigma}$ represent the photon and proton polarizations, respectively. The crossing symmetry implies that the spin-independent amplitude f is an even and the spin-dependent amplitude g is an odd function of ν .

The optical theorem (unitarity) relates the imaginary part of the amplitudes to the total photoabsorption cross sections:

$$\text{Im}f(\nu) = \frac{\nu}{8\pi} [\sigma_{1/2}(\nu) + \sigma_{3/2}(\nu)], \quad (2a)$$

$$\text{Im}g(\nu) = \frac{\nu}{8\pi} [\sigma_{1/2}(\nu) - \sigma_{3/2}(\nu)]. \quad (2b)$$

Here, $\sigma_\lambda(\nu)$ is the doubly polarized cross section with λ representing the combined helicity of the initial γp state. Averaging over the polarization of initial particles gives the unpolarized photoabsorption cross section, $\sigma = \frac{1}{2}(\sigma_{1/2} + \sigma_{3/2})$.

In the present article, we focus on relations involving the spin-independent amplitude f and the unpolarized cross section σ . The Kramers-Kronig relation between these quantities exploits the optical theorem, causality, and crossing symmetry, to yield for the proton [1]:

$$\text{Re}f(\nu) = -\frac{\alpha}{M_p} + \frac{\nu^2}{2\pi^2} \int_0^\infty \frac{d\nu'}{\nu'^2 - \nu^2} \sigma(\nu'), \quad (3)$$

where $\alpha = e^2/4\pi$ is the fine-structure constant, and M_p is the proton mass; the slashed integral denotes the principal-value integration.

We next would like to consider the low-energy expansion of f . At this point, it is important to note that the elastic scattering, i.e., the CS process itself, is one of the photoabsorption processes. The total CS cross section does not vanish for $\nu \rightarrow 0$ but goes to a constant—the Thomson cross section:

$$\sigma(0) = \frac{8\pi\alpha^2}{3M_p^2}. \quad (4)$$

This means Eq. (3) does not admit a Taylor-series expansion around $\nu = 0$ (each coefficient in that expansion is infrared divergent; cf. the Appendix). Such expansion is, nonetheless, important for establishing the polarizability sum rules. We, hence, prefer to take the CS out of the total cross section, i.e.,

$$\sigma(\nu) = \sigma_{\text{CS}}(\nu) + \sigma_{\text{abs}}(\nu), \quad (5)$$

where σ_{abs} can be assumed to be dominated by hadron-production processes, for which there is a threshold at some $\nu_0 > m_\pi$.

The amplitude f can be decomposed accordingly into the elastic and inelastic terms,

$$f(\nu) = f_{\text{el}}(\nu) + f_{\text{inel}}(\nu), \quad (6)$$

$$f_{\text{el}}(\nu) = -\frac{\alpha}{M_p} + \frac{\nu^2}{2\pi^2} \int_0^\infty \frac{d\nu'}{\nu'^2 - \nu^2} \sigma_{\text{CS}}(\nu'), \quad (7)$$

$$f_{\text{inel}}(\nu) = \frac{\nu^2}{2\pi^2} \int_{\nu_0}^\infty \frac{d\nu'}{\nu'^2 - \nu^2} \sigma_{\text{abs}}(\nu'). \quad (8)$$

The details on dealing with f_{el} can be found in the Appendix. In what follows, however, we neglect the contribution from σ_{CS} , as it is suppressed by an extra order of α . Hence, we set $f_{\text{el}}(\nu) = -\alpha/M_p$, as is usually done.

Considering f_{inel} , the low-energy expansion of both sides of Eq. (8) leads to the sum rules for polarizabilities. At the leading order [$O(\nu^2)$], one obtains the Baldin sum rule [2] for the sum of electric (α_{E1}) and magnetic (β_{M1}) dipole polarizabilities:

$$\alpha_{E1} + \beta_{M1} = \frac{1}{2\pi^2} \int_{\nu_0}^\infty d\nu \frac{\sigma_{\text{abs}}(\nu)}{\nu^2}. \quad (9)$$

At $O(\nu^4)$, we obtain “the fourth-order sum rule”:

$$\alpha_{E\nu} + \beta_{M\nu} + \frac{1}{12}(\alpha_{E2} + \beta_{M2}) = \frac{1}{2\pi^2} \int_{\nu_0}^\infty d\nu \frac{\sigma_{\text{abs}}(\nu)}{\nu^4}, \quad (10)$$

which involves the quadrupole polarizabilities α_{E2} , β_{M2} , as well as the leading dispersive contribution to the dipole polarizabilities denoted as $\alpha_{E\nu}$, $\beta_{M\nu}$; see [11] for more details.

Our aim here is to provide an empirical fit of the available data for σ_{abs} and evaluate the various sum rules.

III. FITS OF THE PHOTOABSORPTION CROSS SECTION

The presently available experimental data, together with the results of the empirical analyses MAID and SAID, as well as our fits, are displayed in Fig. 1. In our fitting, we distinguish the following three regions:

- (i) *low energy*, $\nu \in [\nu_0, \nu_1)$,
- (ii) *medium energy*, $\nu \in [\nu_1, 2 \text{ GeV})$,
- (iii) *high energy*, $\nu \in [2 \text{ GeV}, \infty)$,

where ν_0 ($\approx 0.145 \text{ GeV}$) and ν_1 ($\approx 0.309 \text{ GeV}$) are, respectively, the thresholds for the single- and double-pion photoproduction on the proton.

In the *low-energy* region, we use the pion-production ($\pi^+ n$ and $\pi^0 p$) cross sections from the MAID [12] and SAID [14] partial-wave analyses. In our error estimate, we assign a 2% uncertainty on these values.

In the *medium-energy* region, we fit the actual experimental data using a sum of Breit-Wigner resonances and a background. Following [8], we take six Breit-Wigner resonances, each parametrized as

$$\sigma_R(W) = A \frac{\Gamma^2/4}{(W - M)^2 + \Gamma^2/4}, \quad (11)$$

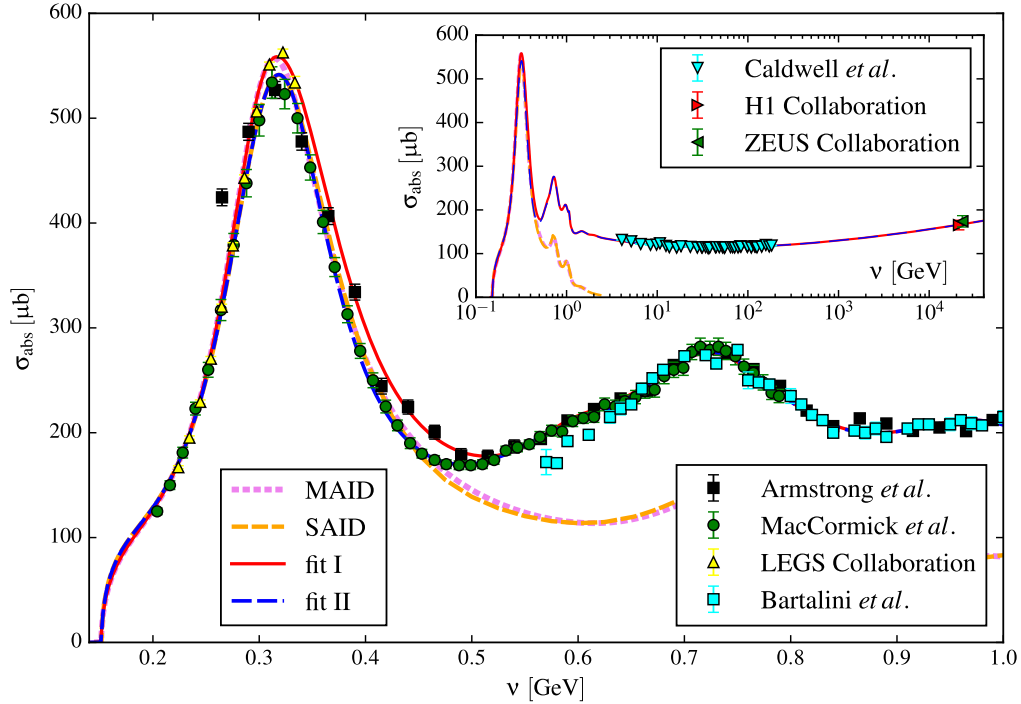


FIG. 1 (color online). Fits of the experimental data for the total photoabsorption cross section on the proton. Fit I is obtained using MAID [12] results below the 2π production and data from LEGS [13] and Armstrong *et al.* [6] above it. Fit II uses SAID [14] and the data of MacCormick *et al.* [15]. Both fits use Bartalini *et al.* [16] and the high-energy data [17–19] displayed in the inset.

where $W = \sqrt{s}$ is the total energy of the γp system. The background function is from [6]:

$$\sigma_B(W) = \sum_{k=-2}^2 C_k (W - W_0)^k, \quad (12)$$

where $W_0 = M_p + m_\pi$ corresponds with the pion photo-production threshold.

Observing a significant discrepancy between SAID and MAID around the $\Delta(1232)$ -resonance peak and a similar

discrepancy between two sets of experimental data, we have made two different fits:

- (I) MAID [12] + LEGS [13] + Armstrong *et al.* [6],
- (II) SAID [14] + MacCormick *et al.* [15].

They are shown in Fig. 1 by the red solid and blue dashed lines, respectively. The corresponding values of parameters are given in Tables I and II. In both fits, we have also made use of the GRAAL 2007 data [16] shown in the figure by light blue squares. These data were not available at the time of the previous sum rule evaluations.

Finally, for the *high-energy region*, we use the standard Regge form [20] (p. 191):

$$\sigma_{\text{Regge}}(W) = c_1 W^{p_1} + c_2 W^{p_2}. \quad (13)$$

For W in GeV and the cross section in μb , we obtain the following parameters (for both of our fits):

TABLE II. Fitting parameters for the background (12) obtained for fits I and II in the resonance region.

	Fit I	Fit II
C_{-2} ($\mu\text{b GeV}^2$)	0.44 ± 0.22	0.26 ± 0.17
C_{-1} ($\mu\text{b GeV}$)	-11.06 ± 3.69	-7.97 ± 2.89
C_0 (μb)	74.38 ± 20.16	57.27 ± 16.09
C_1 ($\mu\text{b GeV}^{-1}$)	22.18 ± 37.71	54.26 ± 31.07
C_2 ($\mu\text{b GeV}^{-2}$)	37.69 ± 21.48	19.51 ± 18.17

TABLE I. Fitting parameters for the resonances (11) obtained for fits I and II.

	M (MeV)	Γ (MeV)	A (μb)
Fit I	1213.6 ± 0.1	117.6 ± 1.9	522.7 ± 17.0
	1412.8 ± 5.9	82.8 ± 26.8	40.1 ± 33.8
	1496.0 ± 2.8	136.5 ± 11.1	161.8 ± 32.4
	1649.4 ± 4.1	135.3 ± 15.3	83.2 ± 22.7
	1697.5 ± 2.6	18.8 ± 12.6	18.2 ± 26.0
	1894.3 ± 15.6	302.0 ± 41.3	31.5 ± 8.7
Fit II	1214.8 ± 0.1	99.0 ± 1.1	502.3 ± 12.3
	1403.9 ± 6.2	118.2 ± 19.6	51.8 ± 23.8
	1496.9 ± 2.1	133.4 ± 9.4	162.0 ± 29.2
	1648.0 ± 4.4	135.2 ± 15.9	83.6 ± 23.8
	1697.2 ± 2.7	21.2 ± 13.2	18.7 ± 25.9
	1893.7 ± 17.4	323.5 ± 45.3	31.7 ± 9.1

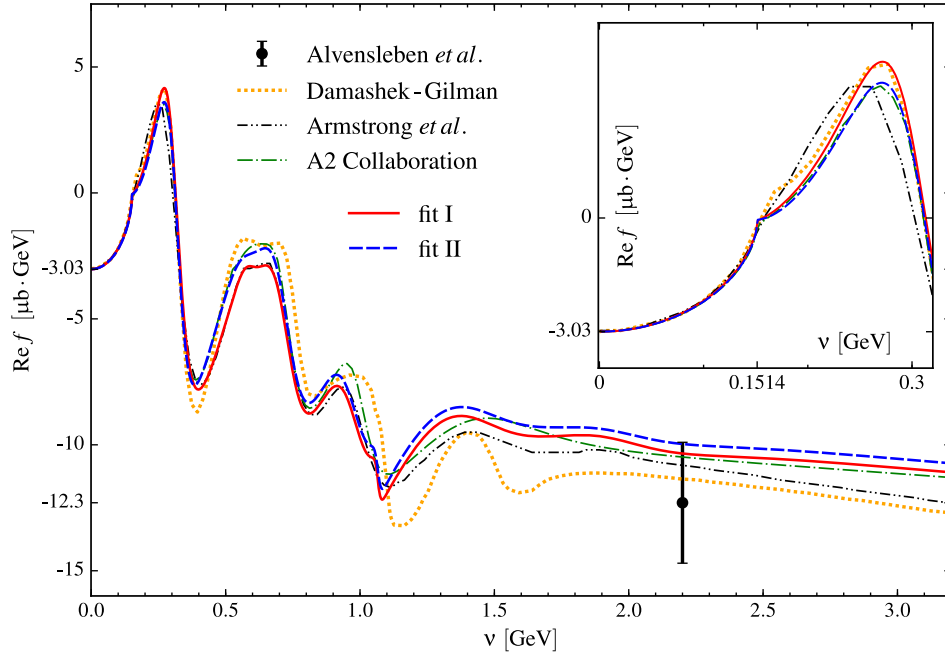


FIG. 2 (color online). Our evaluation of $\text{Re } f$ based on the two fits of the photoabsorption cross section compared with previous evaluations [5,6,9]. The experimental data point is from Ref. [10].

$$c_1 = 62.0 \pm 8.1, \quad c_2 = 126.3 \pm 4.3,$$

$$p_1 = 0.184 \pm 0.032, \quad p_2 = -0.81 \pm 0.12.$$

$$\chi^2 = \sum_i \frac{(\sigma_i^{\text{fit}} - \sigma_i^{\text{exp}})^2}{(\Delta\sigma_i^{\text{exp}})^2} \quad (14)$$

We also tried the high-energy parameterization used in [8] but obtained a worse fit and abandoned it.

The fitting was done with the help of the SCIPY package for PYTHON. The resulting chi-square evaluated as

is of about the same quality for the two fits. In the intermediate region, we obtain $\chi^2/\text{point} = 0.7$ for fit I and $\chi^2/\text{point} = 0.6$ for fit II. In the high-energy region, $\chi^2/\text{point} = 1.2$ in both cases. Again, the low-energy region is not fitted but is borrowed from, respectively, the MAID and SAID analyses.

TABLE III. Empirical evaluations of sum rules and verification of the Kramers-Kronig relation for the proton.

	Baldin (10^{-4} fm^3)	Fourth order (10^{-4} fm^5)	Sixth order ^a (10^{-4} fm^7)	$\text{Re } f(2.2 \text{ GeV})$ ($\mu\text{b GeV}$)
Damashek-Gilman [5]	14.2 ± 0.3			-11.5^{b}
Armstrong <i>et al.</i> [6]				-10.8
Schröder [7]	14.7 ± 0.7	6.4		
Babusci <i>et al.</i> [8]	13.69 ± 0.14			
A2 Collaboration [9]	13.8 ± 0.4			-10.5^{c}
MAID (π chan.) [12]	11.63^{d}			
SAID (π chan.) [14]	11.5^{e}			
This work				
Fit I	14.29 ± 0.27	6.08 ± 0.12	4.36 ± 0.09	-10.35
Fit II	13.85 ± 0.22	6.01 ± 0.11	4.42 ± 0.08	-9.97
Experiment				
Alvensleben <i>et al.</i> [10]				-12.3 ± 2.4

^a $\int_{\nu_0}^{\infty} d\nu \nu^{-6} \sigma_{\text{abs}}(\nu) / (2\pi^2)$

^bInterpolated value.

^cBased on the cross-section parametrization from [21].

^dIntegrated from threshold to $\nu_{\text{max}} = 1.663 \text{ GeV}$.

^eIntegrated from threshold to $\nu_{\text{max}} = 2 \text{ GeV}$.

TABLE IV. Contributions of different regions to the Baldin sum rule for the two fits in Fig. 1.

Fit	$\alpha_{E1} + \beta_{M1} (10^{-4} \text{ fm}^3)$		High energy
	Low energy	Medium energy	
I	6.12 ± 0.12	7.53 ± 0.13	0.64 ± 0.02
II	6.06 ± 0.12	7.15 ± 0.08	0.64 ± 0.02

TABLE V. Contributions of different regions to the fourth-order sum rule for the two fits in Fig. 1.

Fit	$\alpha_{E\nu} + \beta_{M\nu} + \frac{1}{12}(\alpha_{E2} + \beta_{M2})(10^{-4} \text{ fm}^5)$		
	Low energy	Medium energy	High energy
I	4.50 ± 0.09	1.58 ± 0.03	$(219 \pm 8) \times 10^{-5}$
II	4.53 ± 0.09	1.48 ± 0.01	$(219 \pm 8) \times 10^{-5}$

IV. SUM RULE EVALUATIONS

Having obtained the fits of the total photoabsorption cross section σ_{abs} , we evaluate the integrals in Eqs. (8)–(10); the results are presented in Fig. 2 and Table III.

Tables IV and V show contributions of each region to the Baldin and the fourth-order sum rule, respectively. The uncertainty in calculating an integral $I_n = \int d\nu \nu^{-n} \sigma(\nu)$ has been evaluated as follows:

$$\Delta I_n = \sum_i \frac{\Delta \nu_i}{\nu_i^n} \chi_i^2 \Delta \sigma_i^{\text{exp}}, \quad (15)$$

where χ_i^2 is the chi-square at the point i ; cf. Eq. (14).

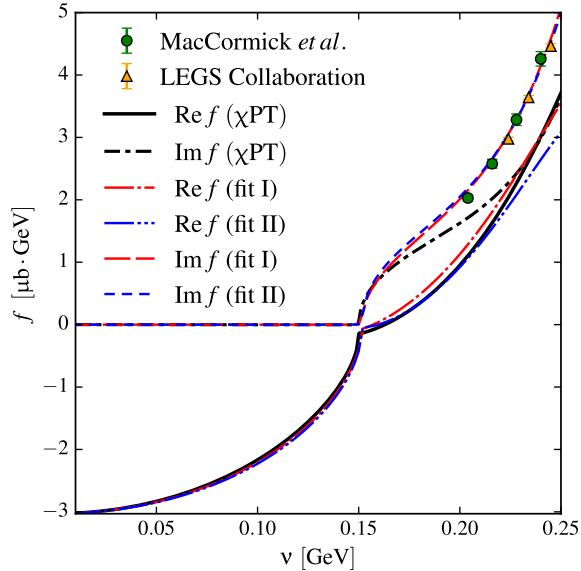


FIG. 3 (color online). Our evaluations of $f(\nu)$ compared to the χ PT calculation of Ref. [22].

The corresponding full results (sum of the three regions) are given in Table III and compared with the results of previous works. In this table, we also give the result for the sixth-order integral and for the full amplitude f at $\nu = 2.2$ GeV. The real part of f is plotted in Fig. 2 over a broad energy range and compared with previous evaluations and the experimental number from the 1973 DESY experiment at 2.2 GeV. Although none of the evaluations really contradicts the experiment, there is a clear tendency to a higher central value.

The new dilepton photoproduction experiments planned at the Mainz Microtron (MAMI) could, perhaps, provide experimental values in the lower-energy range. Obviously, the regions of the extrema [e.g., the $\Delta(1232)$ region or the interval between 0.6 and 0.7 GeV] are most interesting as the different evaluations seem to differ there the most. In the region around 0.6 GeV, for example, one of our evaluations (fit I) is nearly identical with Armstrong's [6], while the other one (fit II) is aligning with DG [5] and the A2 Collaboration [9]. An appropriately precise experiment could tell which of the groups is correct, if any.

Figure 3 shows both the real and imaginary parts of f at lower energies, where they can be compared with a calculation done within chiral perturbation theory (χ PT) [22]. A rather nice agreement between theory and empirical evaluations is observed for energies up to about the pion-production threshold.

For very low energy, this comparison can be made more quantitative by looking at the polarizabilities. While for the

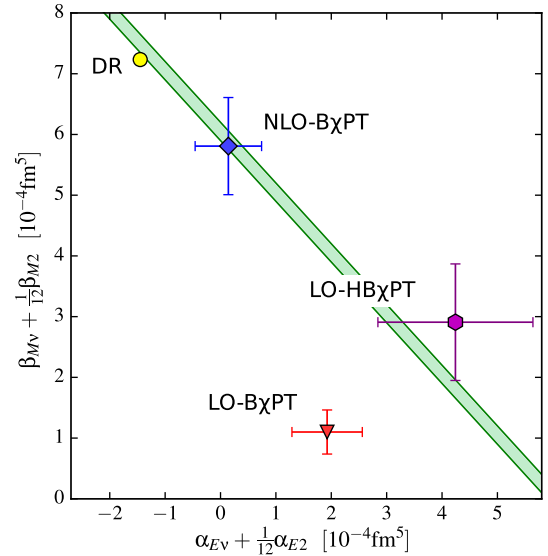


FIG. 4 (color online). The fourth-order sum rule constraint for $\alpha_{E\nu} + \frac{1}{12}\alpha_{E2}$ and $\beta_{M\nu} + \frac{1}{12}\beta_{M2}$ combinations of polarizabilities compared to results from dispersion relation approaches (DR) [11,24], baryon chiral perturbation theory (B χ PT) [25], and heavy baryon chiral perturbation theory (HB χ PT) [26]. The errors of the χ PT derive from our crude estimate of the next-order corrections.

Baldin sum rule the situation was extensively discussed in the literature (cf. [23] for a recent review), the fourth-order sum rule was not studied at all. It can, however, be very useful in unraveling the higher-order polarizabilities, as illustrated by Fig. 4. This is the plot of a combination of proton magnetic polarizabilities versus electric, where the various theory predictions are compared with our fourth-order sum rule evaluation. The band representing the sum rule covers the interval between the two values given in Table III (rows “fit I” and “fit II”). The sum rule clearly provides a model-independent constraint on these polarizabilities and a rather stringent test for the theoretical approaches.

V. CONCLUSION

The fundamental relation between the photon absorption and scattering encompassed in the Kramers-Kronig type of relations allows us to evaluate the forward Compton scattering off protons using the empirical knowledge of the total photoabsorption cross sections. The present database of the unpolarized photoabsorption cross section is not entirely consistent, and so as to reflect that, we obtain two distinct fits to it. The two fits yield slightly different results for the spin-independent amplitude $f(\nu)$ and, hence, for its low-energy expansion characterized by the scalar polarizabilities of the proton. Our two results for the sum of dipole polarizabilities (or Baldin sum rule) correspond nicely with the results of previous evaluations, which too can be separated into two groups: the *old* [5,7], with the value slightly above 14 (in units of 10^{-4} fm^3), and the *new* [8,9], with the value slightly below 14. The 1996 DAPHNE@MAMI experiment [15] superseding the 1972 experiment of Armstrong *et al.* [6] is clearly responsible for this difference. Neglecting the older data in favor of the newer ones yields the lower value of the Baldin sum rule and vice versa. While one can take a preference in one of the two fits and the corresponding results, we prefer to think of their difference as a systematic uncertainty in the present evaluation of the polarizabilities and of the forward spin-independent amplitude of the proton.

As far as polarizabilities are concerned, only the Baldin sum rule is appreciably affected by the inconsistency in the photoabsorption database. Nevertheless, the two results (fit I and II in Table III) are not in conflict with each other, given the overlapping error bars. It is customary to take a statistical average¹ over our two values for the Baldin sum rule we obtain $\alpha_{E1}^{(p)} + \beta_{M1}^{(p)} = (14.0 \pm 0.2) \times 10^{-4} \text{ fm}^3$. The error

¹For the weighted average, $\bar{x} \pm \bar{\sigma}$, over a set $\{x_i \pm \sigma_i\}$, we use [27] (p. 120):

$$\bar{x} = \frac{\sum_i x_i / \sigma_i^2}{\sum_j 1 / \sigma_j^2}, \quad \bar{\sigma} = \left(\frac{\sum_i (x_i - \bar{x})^2 / \sigma_i^2}{\sum_j 1 / \sigma_j^2} \right)^{1/2}.$$

bar here does not directly include the aforementioned systematic uncertainty of the cross section database. However, since the two results are fairly well surmised by the weighted average, the latter should be less prone to the systematic uncertainty of the database.

We have presented a first study of the sum rule involving the quadrupole polarizabilities, Eq. (10), here referred to as the fourth-order sum rule. Our weighted average value for this sum rule in the proton case is $6.04(4) \times 10^{-4} \text{ fm}^5$. It agrees very nicely with the state-of-the-art calculations of these polarizabilities based on fixed- t dispersion relations and chiral perturbation theory; see Fig. 4. We note that, while the calculations demonstrate significant differences in the values of individual higher-order polarizabilities, these differences apparently cancel out from the forward combination of these polarizabilities which enters the sum rule.

In the subsequent paper, we will discuss the evaluation of the forward *spin-dependent* amplitude $g(\nu)$ and related sum rules for the forward spin polarizabilities of the proton. The knowledge of the two amplitudes will allow us to reconstruct the observables for the proton Compton scattering at zero angle.

ACKNOWLEDGMENTS

We thank Jürgen Ahrens for kindly supplying us with a database of total photoabsorption cross sections. This work was supported by the Deutsche Forschungsgemeinschaft (DFG) through the Collaborative Research Center SFB 1044 (The Low-Energy Frontier of the Standard Model) and the Graduate School DFG/GRK 1581 (Symmetry Breaking in Fundamental Interactions).

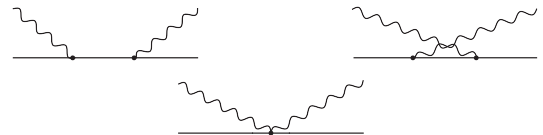


FIG. 5. Tree-level CS diagrams.

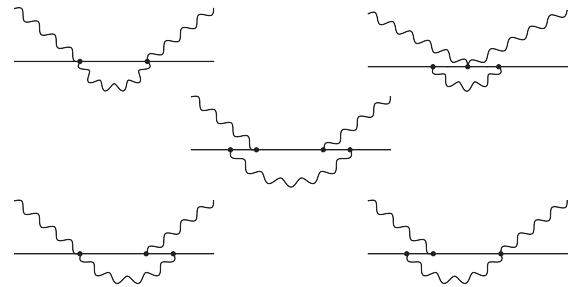


FIG. 6. One-loop graphs contributing to the forward CS. Diagrams obtained from these by crossing of the photon lines are included too.

APPENDIX: SUM RULES FOR ELASTIC CONTRIBUTION IN SCALAR QED

Consider the elastic forward scattering of a photon with momentum q from a charged spinless particle with four-momentum p and mass M . In the forward direction ($t = 0$), this process is completely described by a single amplitude $f(\nu)$. The tree-level QED calculation (Fig. 5) yields immediately $f^{(1)}(\nu) = -\alpha/M$, where we have chosen the normalization of this amplitude to coincide with the analogous amplitude for the spin-1/2 case [see Eq. (1)]; the superscript indicates the order of α .

$$f^{(2)}(\nu) = \frac{\alpha^2}{2\pi M} \left\{ \frac{\pi^2 M(M-\nu) + 12\nu^2}{6\nu^2} + \frac{8\nu^2}{(M^2 - 4\nu^2)} \ln \frac{2\nu}{M} + \frac{M(M+\nu)}{\nu^2} \ln \frac{2\nu}{M} \ln \left(1 + \frac{2\nu}{M} \right) + \frac{M}{\nu^2} \left[(M+\nu) \text{Li}_2 \left(-\frac{2\nu}{M} \right) - (M-\nu) \text{Li}_2 \left(1 - \frac{2\nu}{M} \right) \right] \right\} + \frac{i}{4\pi} \nu \sigma^{(2)}(\nu), \quad (\text{A1})$$

where $\text{Li}_2(x)$ is the dilogarithm, and $\sigma^{(2)}(\nu)$ is the total CS cross section arising at the tree level (cf. Fig. 5),

$$\sigma^{(2)}(\nu) = \frac{2\pi\alpha^2}{\nu^2} \left\{ \frac{2(M+\nu)^2}{M^2 + 2M\nu} - \left(1 + \frac{M}{\nu} \right) \ln \left(1 + \frac{2\nu}{M} \right) \right\}. \quad (\text{A2})$$

We note that in the low-energy limit, it reproduces the Thomson cross section: $\sigma^{(2)}(0) = 8\pi\alpha^2/3M^2$, a result that is unaltered by loop corrections, i.e., $\sigma(0) = \sigma^{(2)}(0)$.

As the total photoabsorption cross section to this order in α is given entirely by the tree-level CS cross section, the fact that $\text{Im}f^{(2)}(\nu) = \nu\sigma^{(2)}(\nu)/4\pi$ coincides in this case with the statement of the optical theorem. We have also checked that the one-loop amplitude satisfies the once-subtracted dispersion relation:

$$f^{(2)}(\nu) = \frac{\nu^2}{2\pi^2} \int_0^\infty d\nu' \frac{\sigma^{(2)}(\nu')}{\nu'^2 - \nu^2 - i0^+}, \quad (\text{A3})$$

and, hence, the full amplitude, $f^{(1)} + f^{(2)}$, indeed enjoys the Kramers-Kronig relation given in Eq. (3).

Now, the whole point of this exercise is to understand the low-energy expansion and, thus, the polarizability sum rules in the case when the photoabsorption cross section is not vanishing at $\nu = 0$. Expanding the real part of Eq. (A3) around $\nu = 0$, we find

$$\begin{aligned} & \frac{\alpha^2}{\pi M} \left(\frac{1 + 24 \ln \frac{2\nu}{M}}{9M^2} \nu^2 + \frac{8(14 + 330 \ln \frac{2\nu}{M})}{225M^4} \nu^4 \right. \\ & \quad \left. + \frac{4(17 + 616 \ln \frac{2\nu}{M})}{49M^6} \nu^6 + \dots \right) \\ &= \frac{1}{2\pi^2} \sum_{n=1}^\infty \nu^{2n} \int_0^\infty d\nu' \frac{\sigma^{(2)}(\nu')}{\nu'^{2n}}. \end{aligned} \quad (\text{A4})$$

Next, we consider the one-loop corrections. Figure 6 shows the one-particle-irreducible diagrams appearing in scalar QED. The corresponding one-particle-reducible diagrams vanish in forward direction, due to the transversality of the photon polarization vector ϵ with respect to any of the four momenta, i.e., $q \cdot \epsilon = 0 = p \cdot \epsilon$.

Renormalization of these diagrams amounts to subtracting their contribution at $\nu = 0$. We, thus, find the following expression for the renormalized amplitude at order $O(\alpha^2)$:

Hence, the coefficients diverge in the infrared. However, there is an apparent mismatch: they are logarithmically divergent on one side and power divergent on the other. To match the sides exactly at each order of ν , thus, defining the sum rules for “quasistatic” polarizabilities, we subtract all the power divergences on the right-hand side (rhs) and regularize both sides with the same infrared cutoff (equal to ν):

$$\begin{aligned} & \frac{\alpha^2}{\pi M} \left(\frac{1 + 24 \ln \frac{2\nu}{M}}{9M^2} \nu^2 + \frac{8(14 + 330 \ln \frac{2\nu}{M})}{225M^4} \nu^4 + \dots \right) \\ &= \frac{1}{2\pi^2} \sum_{n=1}^\infty \nu^{2n} \int_\nu^\infty d\nu' \frac{\sigma^{(2)}(\nu') - \sum_{k=0}^{2(n-1)} \frac{1}{k!} \frac{d^k \sigma^{(2)}(\nu')}{d\nu'^k} \Big|_{\nu=0} \nu'^k}{\nu'^{2n}}. \end{aligned} \quad (\text{A5})$$

Both sides are now identical at each order of ν . This is nontrivial, at least for the analytic terms; the logs are fairly easily obtained from the nonregularized rhs in Eq. (A4); cf. [28].

Extending these arguments to all orders in α , we find that the proper low-energy expansion for the “elastic” part of the amplitude [see Eq. (7)] reads as

$$f_{\text{el}}(\nu) = -\frac{\alpha}{M} + \frac{1}{2\pi^2} \sum_{n=1}^\infty \nu^{2n} \int_\nu^\infty d\nu' \frac{\sigma(\nu') - \bar{\sigma}_n(\nu')}{\nu'^{2n}}, \quad (\text{A6})$$

where σ is the total cross section of Compton scattering and $\bar{\sigma}_n$ are the infrared subtractions:

$$\bar{\sigma}_n(\nu') \equiv \sum_{k=0}^{2(n-1)} \frac{1}{k!} \left. \frac{d^k \sigma(\nu)}{d\nu^k} \right|_{\nu=0} \nu'^k. \quad (\text{A7})$$

Now we can, for instance, formulate the Baldin sum rule for the elastic contribution to the dipole polarizabilities. By definition

$$f_{\text{el}}(\nu) = -\alpha/M + (\alpha_{E1} + \beta_{M1})_{\text{el}} \nu^2 + O(\nu^4), \quad (\text{A8})$$

and hence, matching it with the rhs of Eq. (A6), we obtain

$$(\alpha_{E1} + \beta_{M1})_{\text{el}} = \frac{1}{2\pi^2} \int_{\nu}^{\infty} d\nu' \frac{\sigma(\nu') - \sigma(0)}{\nu'^2}. \quad (\text{A9})$$

In our scalar QED example, where σ is the tree-level cross section $\sigma^{(2)}$, we obtain

$$(\alpha_{E1}^{(2)} + \beta_{M1}^{(2)})_{\text{el}} = \frac{\alpha^2}{9\pi M^3} \left(1 + 24 \ln \frac{2\nu}{M} \right), \quad (\text{A10})$$

which, of course, reproduces the one-loop result [cf. the first term in the expansion of $f^{(2)}$ in Eq. (A5)].

-
- [1] M. Gell-Mann, M. L. Goldberger, and W. E. Thirring, *Phys. Rev.* **95**, 1612 (1954).
[2] A. M. Baldin, *Nucl. Phys.* **18**, 310 (1960).
[3] S. B. Gerasimov, *Yad. Fiz.* **2**, 598 (1965); *Sov. J. Nucl. Phys.* **2**, 430 (1966).
[4] S. D. Drell and A. C. Hearn, *Phys. Rev. Lett.* **16**, 908 (1966).
[5] M. Damashek and F. J. Gilman, *Phys. Rev. D* **1**, 1319 (1970).
[6] T. A. Armstrong *et al.*, *Phys. Rev. D* **5**, 1640 (1972).
[7] U. E. Schröder, *Nucl. Phys.* **B166**, 103 (1980).
[8] D. Babusci, G. Giordano, and G. Matone, *Phys. Rev. C* **57**, 291 (1998).
[9] V. Olmos de Leon *et al.*, *Eur. Phys. J. A* **10**, 207 (2001).
[10] H. Alvensleben *et al.*, *Phys. Rev. Lett.* **30**, 328 (1973).
[11] D. Babusci, G. Giordano, A. I. L'vov, G. Matone, and A. M. Nathan, *Phys. Rev. C* **58**, 1013 (1998).
[12] D. Drechsel, S. S. Kamalov, and L. Tiator, *Eur. Phys. J. A* **34**, 69 (2007); MAID, <http://www.kph.uni-mainz.de/MAID/>.
[13] A. M. Sendorfi *et al.*, Report No. BNL-64382, 1996.
[14] R. L. Workman, M. W. Paris, W. J. Briscoe, and I. I. Strakovsky, *Phys. Rev. C* **86**, 015202 (2012); G. Blanpied *et al.* (The LEGS Collaboration), *Phys. Rev. Lett.* **79**, 4337 (1997).
[15] M. McCormick *et al.*, *Phys. Rev. C* **53**, 41 (1996).
[16] O. Bartalini *et al.*, *Phys. At. Nucl.* **71**, 75 (2008).
[17] D. O. Caldwell *et al.*, *Phys. Rev. Lett.* **40**, 1222 (1978).
[18] S. Aid *et al.* (H1 Collaboration), *Z. Phys. C* **69**, 27 (1995).
[19] S. Chekanov *et al.* (ZEUS Collaboration), *Nucl. Phys.* **B627**, 3 (2002).
[20] R. M. Barnett *et al.* (Particle Data Group), *Phys. Rev. D* **54**, 1 (1996).
[21] J. Ahrens (private communication).
[22] V. Lensky and V. Pascalutsa, *Eur. Phys. J. C* **65**, 195 (2010).
[23] H. W. Griesshammer, J. A. McGovern, D. R. Phillips, and G. Feldman, *Prog. Part. Nucl. Phys.* **67**, 841 (2012).
[24] D. Drechsel, B. Pasquini, and M. Vanderhaeghen, *Phys. Rep.* **378**, 99 (2003).
[25] V. Lensky, J. A. McGovern, and V. Pascalutsa, [arXiv:1510.02794](https://arxiv.org/abs/1510.02794).
[26] B. R. Holstein, D. Drechsel, B. Pasquini, and M. Vanderhaeghen, *Phys. Rev. C* **61**, 034316 (2000).
[27] L. G. Parratt, *Probability and Experimental Errors in Science* (John Wiley & Sons, New York, 1961).
[28] B. R. Holstein, V. Pascalutsa, and M. Vanderhaeghen, *Phys. Rev. D* **72**, 094014 (2005).